

# Stochastic identities for random isotropic fields

A.S. Il'yn<sup>1,2</sup>, A.V. Kopyev<sup>1</sup>, V.A. Sirota<sup>1</sup>, K.P. Zybin<sup>1,2</sup>

<sup>1</sup> *P.N. Lebedev Physical Institute of RAS, 119991, Leninskij pr. 53, Moscow, Russia*

<sup>2</sup> *National Research University Higher School of Economics, 101000, Myasnitskaya 20, Moscow, Russia*

This letter presents new nontrivial stochastic identities for random isotropic second rank tensor fields. They can be considered as markers of statistical isotropy in turbulent flows of any nature. The case of axial symmetry is also considered. We confirm the validity of the identities using different direct numerical simulations of turbulent flows.

## INTRODUCTION

It is known that the flow of viscous fluid is unstable at high Reynolds numbers. In three-dimensional hydrodynamic flow after some time the velocity field becomes chaotic and the spectrum of its pulsations extends from the integral to the dissipative (Kolmogorov) scale [1, 2]. This phenomenon is called fully developed turbulence. One of Kolmogorov's hypotheses states that random differences in velocity fluctuations at two arbitrary points  $\delta \mathbf{u}$  in such a flow are statistically homogeneous and isotropic if the points are located quite far from the boundaries of the flow [3]. The verification of the hypothesis in a specific stream remains a challenge [4].

From mathematical point of view, the isotropy of the flow means that the probability measure of  $\delta \mathbf{u}$  is invariant with respect to the group of space motions (the semi-direct product of parallel transport and orthogonal transformations  $\mathbb{R} \times O(3)$ ):

$$\mathbf{u}(t, \mathbf{r}) \rightarrow \mathbf{u}(t, \mathbf{R}^{-1}(\mathbf{r} - \mathbf{a}) + \mathbf{a}), \quad \mathbf{a} \in \mathbb{R}^3, \mathbf{R} \in O(3)$$

Let us now consider tensor fields that are functionally dependent on the velocity field. For instance, it can be a velocity gradients field usually studied in the theory of turbulence [5, 6]:

$$A_{kp} = \frac{\partial u_k}{\partial r_p},$$

or a magnetic induction gradients field in magneto-hydrodynamic turbulence [7, 8]:

$$H_{kp} = \frac{\partial B_k}{\partial r_p},$$

or a field of second derivatives of a scalar  $\phi$ , which is studied in the theory of advection of scalar fields [9–11]:

$$\Phi_{kp} = \frac{\partial^2 \phi}{\partial r_k \partial r_p}$$

In the absence of external factors that could affect the field dynamics, these advected fields become statistically (locally) isotropic in a fully developed turbulent flow; all the fields have finite correlation lengths, and unlike, e.g., ferromagnetics, there can be no spontaneous symmetry breaking in turbulent media.

So, local isotropy is an inherent property of fully developed turbulence, even though statistical homogeneity and stationarity can be violated. If the flow is, in addition, homogenous and/or stationary, then the corresponding ergodic theorem is valid, and the mathematical expectations of every function of the field can be calculated or measured by taking spatial or time average.

Isotropy leads to the existence of the so-called stochastic identities, i.e. some functions of the tensor components with universal mathematical expectations that do not change during evolution. The simplest example of such an identity is the following:

$$\left\langle \left( \frac{\delta u_1}{\delta u} \right)^2 \right\rangle = \left\langle \left( \frac{\delta u_2}{\delta u} \right)^2 \right\rangle = \left\langle \left( \frac{\delta u_3}{\delta u} \right)^2 \right\rangle = \frac{1}{3} \quad (1)$$

This identity is trivial. Moreover, it remains true not only for isotropic fields, but also for the fields with probability measure invariant only under coordinate axes permutations (and not isotropic).

This letter presents far less trivial stochastic identities that can be used as markers of isotropy for arbitrary second rank tensors. We focus on the three dimensional case; however, they can as well be applied to spaces of any dimension.

## LDU DECOMPOSITION OF MATRICES

The human experience shows that when trying to better understanding of a statement it should be formulated in a broadest way possible. Therefore, it would not hurt to consider a Euclidean space with arbitrary dimension  $d$ .

Consider arbitrary second rank tensors  $\mathbf{A}$  and symmetric positive-definite quadratic form  $\mathbf{\Gamma} = \mathbf{A}^T \mathbf{A}$ . In accordance with the Gauss (lower-diagonal-upper, LDU) decomposition, in the given basis its matrix can be presented in the form:

$$\mathbf{\Gamma} = \mathbf{Z}^T \mathbf{D}^2 \mathbf{Z}, \quad (2)$$

where  $\mathbf{D} = \text{diag}\{D_1, \dots, D_d\}$ ,  $D_i > 0$ ,  $\mathbf{Z}$  is an upper-triangular matrix with units on the main diagonal.

It is important to note that the coefficients  $D_i$  are not equal to the eigenvalues of  $\mathbf{\Gamma}$ , except for the case of a diagonal matrix. Unlike the eigenvalues, they are not

universal characteristics of the quadratic form: the set  $\{D_i\}$  depends on the chosen basis.

It follows from (2) that

$$D_k^2 = s_k^2/s_{k-1}^2, \quad (3)$$

where  $s_k^2$  is the  $k$ -order leading principal minor of  $\mathbf{\Gamma}$ .

### SYMMETRY PROPERTIES OF $\{D_i\}$ FOR ISOTROPIC RANDOM TENSORS

Let now  $\mathbf{A}$  be random, and let its probability measure be invariant under the rotation in the  $p, p+1$  plane where  $p \in \{1, \dots, d-1\}$ . This means that the probability density  $\rho(\mathbf{A})$  satisfies the identity

$$\rho(\mathbf{A}) = \rho(\mathbf{O}_p^{-1} \mathbf{A} \mathbf{O}_p), \quad (4)$$

where  $\mathbf{O}_p$  is a rotation in the  $p, p+1$  plane. Let  $m_1, \dots, m_d$  be an arbitrary set of real numbers. Then, as it was shown in [12], the correlator

$$C(m_1, \dots, m_d) = \langle D_1^{m_1+1} \dots D_d^{m_d+d} \rangle \quad (5)$$

is symmetric with respect to the pair permutation  $m_p \leftrightarrow m_{p+1}$ . This is a consequence of some nontrivial symmetric property of elliptic integrals, which appear as a result of integration over the  $\text{SO}(2)$  subgroup of  $\text{SO}(d)$ .

Any permutation  $\{\pi(k)\}$  can be represented as a composition of pair permutations of adjacent numbers; thus, for isotropic probability density

$$\rho(\mathbf{A}) = \rho(\mathbf{O}^{-1} \mathbf{A} \mathbf{O}), \forall \mathbf{O} \in O(d), \quad (6)$$

the correlator (5) is symmetric with respect to any permutation  $m_1, \dots, m_d \rightarrow m_{\pi(1)}, \dots, m_{\pi(d)}$ .

### STOCHASTIC IDENTITIES

Substituting  $m_k = -k$  in (5), one obtains

$$1 = \langle D_1^{1-\pi(1)} \dots D_d^{d-\pi(d)} \rangle \quad \forall \{\pi(k)\} \quad (7)$$

By means of (3) we express (7) in terms of the leading principal minors:

$$\langle s_1^{\pi(2)-\pi(1)-1} \dots s_{d-1}^{\pi(d)-\pi(d-1)-1} s_d^{d-\pi(d)} \rangle = 1, \forall \pi(k) \quad (8)$$

These identities are valid for arbitrary isotropic probability measures at any given time. Their existence is entirely due to the geometric properties of  $O(d)$ , regardless of the dynamics of the field.

From geometric point of view,  $s_k$  describe the transformation of infinitesimal segment/square/hypersquare... under the action of  $\mathbf{A}$ . So, the identities can be interpreted as (stochastic) relations between transformations of hypervolumes of different dimensions (see [12]

and Supplemental materials for more detailed consideration).

Now, we focus on the most practically important case  $d = 3$ . From (8) we get five nontrivial identities (as many as there are nontrivial permutations):

TABLE I: Stochastic identities for isotropic three-dimensional flows. The first two identities are valid for flows with stochastic axial symmetry (1st and 3rd axis, respectively).

Permutation	Stochastic identity
132	$\langle s_1 s_2^{-2} s_3 \rangle = 1$
213	$\langle s_1^{-2} s_2 \rangle = 1$
321	$\langle s_1^{-2} s_2^{-2} s_3^2 \rangle = 1$
231	$\langle s_2^{-3} s_3^2 \rangle = 1$
312	$\langle s_1^{-3} s_3 \rangle = 1$

We note that symmetry of (5) and the relations (7), (8) are not just a result of the change of the axes numbers (as in (1)). Actually, such a change of numbers would not just exchange the values of  $D_i$ : it would change them essentially. The existence of the identities is due to the existence of continuous (not discrete) symmetry.

On the other hand, since the set  $\{D_i\}$  is not invariant under the rotation of the basis, the identities (8) written in different coordinate frames are essentially different: changing the frame, one gets new identities. Namely, let us choose some basis and write down the identities (8). Let us now take some rotated basis and write one of the identities (8) in this new coordinate frame. Then we express the components  $\Gamma'_{ij}$  of the 'new' matrix in terms of the first matrix  $\mathbf{\Gamma}$ , and the obtained identity is functionally independent on the previous five (in the sense that the expressions under the averaging brackets are linearly independent, and there is no relation between them that would be valid for all realizations). This way we get five continuous three-parametric (by the number of rotations) sets of stochastic identities describing the isotropic random tensor.

Returning to the case of arbitrary dimension, we find  $(d! - 1)$  continuous families of identities, each of them being  $d(d-1)/2$ -parametric. Geometrical meaning of these families is discussed in Supplemental Material 1

Below, we illustrate this idea by applying it to the case of axially symmetric flow.

### AXIAL SYMMETRY

Axisymmetric flows are found in turbulent jets [13], channel flows [14], jets that are observed in astrophysical objects [15], etc.

Consider a random tensor that is not completely isotropic but has axial stochastic symmetry, i.e., its probability measure is invariant with respect to rota-

tion around one direction. Choose the coordinate frame in such a way that the selected direction coincides with the first axis. As follows from the reasoning between (4) and (5), the first identity in Table 1 still holds in this case ( $p = 2$  in (4)). Thus, we get

$$\langle s_1 s_2^{-2} s_3 \rangle = 1$$

Now we take, e.g., the coordinate frame with the basis vectors  $\mathbf{e}'_1 = \mathbf{e}_1$ ,  $\mathbf{e}'_2 = \mathbf{e}_3$ ,  $\mathbf{e}'_3 = -\mathbf{e}_2$ . We can express the new components  $\Gamma'_{ij}$  in terms of the primary frame: then,  $s'_1 = s_1$ ,  $s'_3 = s_3$ ,  $s'^2_2 = m_{13}$  where  $m_{ij}$  is the principal 2-rank minor obtained from  $\Gamma$  by preserving the rows and columns with numbers  $i, j$ . Axis 1' is still the axis of symmetry, so we obtain one more equality:

$$\langle s'_1 s'^{-2}_2 s'_3 \rangle = \langle s_1 s_3 / m_{13} \rangle = 1,$$

which contains principal and not only leading principle minors.

Rotating the frame by different angles around the first axis, one would get new identities; they would contain different combinations of the components of  $\Gamma$  (not only minors).

Furthermore, we take one more coordinate frame in such a way that the axis of symmetry is the third coordinate axis: say,  $\mathbf{e}''_1 = \mathbf{e}_2$ ,  $\mathbf{e}''_2 = \mathbf{e}_3$ ,  $\mathbf{e}''_3 = \mathbf{e}_1$ . Then the same consideration of (4) with  $p = 1$  shows that the second identity of Table 1 is valid. Returning back to the primary frame we get

$$\langle s''^{-2}_1 s''_2 \rangle = \langle (\Gamma_{22})^{-1} \sqrt{m_{23}} \rangle = 1,$$

The rotation of the second coordinate frame around the direction of symmetry (i.e., its third axis) produces one more continuous family of identities.

Now, let  $\mathbf{e}_2$  be the direction of axial symmetry. No one of the identities listed in Table 1 holds in this case, since both rotations  $\mathbf{O}_1$  and  $\mathbf{O}_2$  violate the symmetry. However, choosing the coordinate frame  $\{\mathbf{e}\}''_i$  we get the axial symmetry about the new  $x''$  axis, so

$$\langle s''^{-2}_1 s''^{-2}_2 s''_3 \rangle = \langle \sqrt{\Gamma_{22} m_{23}^{-1}} s_3 \rangle = 1$$

In the frame with basis vectors  $\{\mathbf{e}\}'_i$ , the direction of symmetry becomes the  $z'$  axis, and the second line in Table 1 comes into play:

$$\langle s'^{-2}_1 s'^{-2}_2 \rangle = \langle s_1^{-2} \sqrt{m_{13}} \rangle = 1$$

Of course, for each of these cases, one can additionally rotate the coordinate frame around the symmetry axis, and obtain more identities.

So, for any axially symmetric flow there are two continuous one-parametric families of identities.

We would like to note the difference between rotation of the coordinate frame and rotation  $O_p$  in (4)-(5). In

whatever frame the invariance (4) holds, one gets the corresponding identity.

For illustration and for further reference, we collect several identities for each axial symmetry in Table 2: only the ones that are obtained by rotating the frame in coordinate planes by  $90^\circ$ .

TABLE II: The averages that are equal to 1 for axially symmetric tensors.

Coordinates frame: basis vectors	axis of symmetry		
	x	y	z
$(\mathbf{e}_1, \mathbf{e}_2, \mathbf{e}_3)$	$\langle s_1 s_2^{-2} s_3 \rangle$	-	$\langle s_1^{-2} s_2 \rangle$
$(\mathbf{e}_1, \mathbf{e}_3, -\mathbf{e}_2)$	$\langle s_1 m_{13}^{-1} s_3 \rangle$	$\langle s_1^{-2} \sqrt{m_{13}} \rangle$	-
$(\mathbf{e}_2, \mathbf{e}_3, \mathbf{e}_1)$	$\langle \Gamma_{22}^{-1} \sqrt{m_{23}} \rangle$	$\langle \sqrt{\Gamma_{22} m_{23}^{-1}} s_3 \rangle$	-
$(\mathbf{e}_2, -\mathbf{e}_1, \mathbf{e}_3)$	-	$\langle \sqrt{\Gamma_{22} s_2^{-2}} s_3 \rangle$	$\langle \Gamma_{22}^{-1} s_2 \rangle$
$(\mathbf{e}_3, \mathbf{e}_1, \mathbf{e}_2)$	-	$\langle \sqrt{m_{13} \Gamma_{33}^{-1}} \rangle$	$\langle \sqrt{\Gamma_{33} m_{13}^{-1}} s_3 \rangle$
$(\mathbf{e}_3, -\mathbf{e}_2, \mathbf{e}_1)$	$\langle \Gamma_{33}^{-1} \sqrt{m_{23}} \rangle$	-	$\langle \sqrt{\Gamma_{33} m_{23}^{-1}} s_3 \rangle$

## APPLICATION TO VELOCITY GRADIENTS IN NAVIER-STOKES TURBULENCE

To illustrate the theory, we apply it to the results of numerical simulations of incompressible turbulent flow. We consider two different cases: isotropic turbulence and channel flow.

The direct numerical simulation (DNS) data is provided by the Johns Hopkins Turbulence Databases [16, 17]. The DNS of forced isotropic turbulence was performed on a  $1024^3$  periodic grid, using a pseudo-spectral parallel code. It reaches the Taylor-scale Reynolds number that fluctuates around  $R_\lambda \sim 433$ . The channel flow DNS data contain a turbulent flow at a friction velocity Reynolds number  $R_\tau \sim 1000$  within a computational domain of  $L_x \times L_y \times L_z = 8\pi h \times 2h \times 3\pi h$ , where  $h$  denotes the channel half-height and  $x, y, z$  correspond to the streamwise, wall-normal, and spanwise direction, respectively. The numerical grid contains  $N_x \times N_y \times N_z = 2048 \times 512 \times 1536$  grid points. Periodic boundary conditions are applied in the longitudinal and transverse directions, and no-slip conditions at the top and bottom walls.

We refer the interested reader to the original publications of [16–18] for a comprehensive data description.

From the DNS we derive the velocity gradients tensor  $A_{ij} = u_i / r_j$ , construct the symmetric, positive definite matrix  $\Gamma = A^T A$  and calculate the left-hand sides of the identities listed in Table 1. We use the spacial average in-

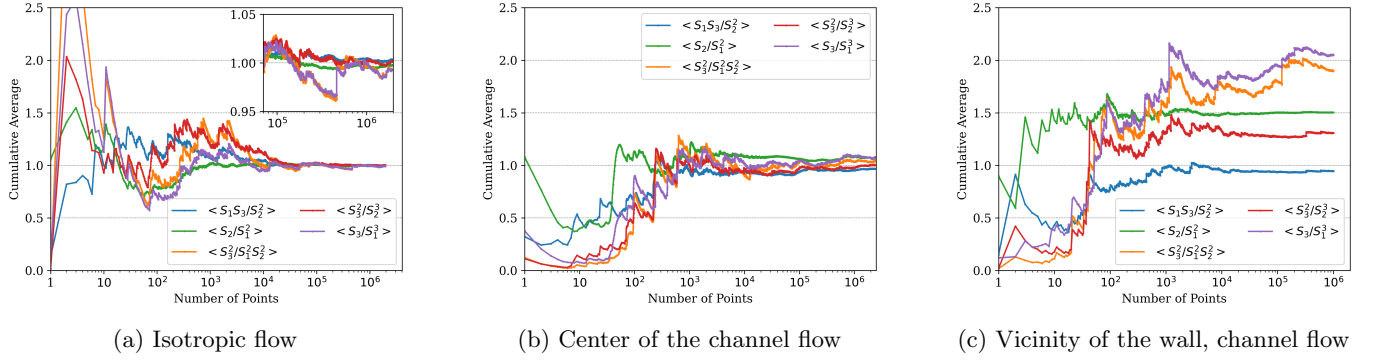


FIG. 1: Saturation of cumulative averages for the five left-hand sides of the identities (Table 1). The blue line corresponds to the identity that holds in the case of stochastic ( $x$ )-axial symmetry.

stead of the mathematical expectation, taking advantage of the finiteness of the correlation length.

We derive each of the averages as a function of number of points (see Fig.1) for three different cases: (a) isotropic turbulence ( $126^3$  points at  $t = 3.3$  evenly spaced in the computed domain), (b) centre of the channel ( $2.4 \times 10^6$  points in the center plane  $y = 0$  at  $t = 3.3$ ), (c) in the channel near the wall ( $10^6$  randomly distributed points in a domain near the wall  $y \in [0.9, 0.95]$  at  $t = 3.3$ ).

One can see that, indeed, all the averages converge well to definite values; for isotropic flow the limits of all the sequences are practically equal to unity, which confirms the identities. Note that the average  $\langle s_2 / s_1^2 \rangle$ , which contains small power of velocity gradient components in the denominator, converges very quickly, while the  $\langle s_3^2 / s_1^2 s_2^2 \rangle$ , which has high power of the denominator, takes much longer time to converge.

In the center of the channel all the averages are also close to unity; this confirms that the turbulence is nearly isotropic, in accordance with the Kolmogorov hypothesis.

As the distance from the center plane  $y = 0$  increases and we approach the wall, all the averages deviate from 1. However, the axial symmetry still holds much better than the others: deviation of  $\langle s_1 s_2^{-2} s_3 \rangle$  from 1 remains at the level of less than 0.1 while the deviation of other averages is of the order of 1.

The graphs also provide an illustration of intermittency of the flow. Indeed, one can see that the values of the averages change sharply, stepwise; these are the rare intermittent events. Moreover, in isotropic flow these rare events are essentially the ones that bring the cumulative average back to unity: the identities, to large extent, hold due to rather rare events.

The profile of the averages as a function of the distance from the wall is presented in Fig. 2. We add two more averages from Table II to those from Table I, to trace the possible presence of  $y$ -axial symmetry. The three regions indicated in the figure correspond to the turbulent, buffer and viscous layers. The boundaries of the zones are determined by the behavior of the mean velocity pro-

file [17].

One can see that deeply inside the turbulent layer all the averages are close to unity, while near the buffer layer they start to change.

The behavior of the first average in Table 1, the one that preserves in the case of axial symmetry around the  $x$  axis, remains the most stable inside the turbulent layer. Its deviation from 1 remains quite small even at the bound of the buffer layer, where the deviations of the other averages are many times more.

The behavior of the averages in the viscous sublayer is close to a power-law. The two averages that reflect the symmetry around the  $y$  axis (the axis normal to the wall) deviate from 1 much less than the others; they stop growing in the buffer layer, and remain almost constant near the wall. This indicates that, although in the viscous layer no symmetry survives, still the symmetry with respect to the wall-normal direction violates less than the others. The value  $\langle s_1^{-2} s_2^{-2} s_3^2 \rangle$  is also much smaller than the others, but it is not associated with any axial symmetry: it is merely one of the averages that must be equal to unity in isotropic flows. We suppose that its moderate behavior near the wall is related to the crucial role of a shear flow; below we demonstrate the arguments in favor of this supposition.

To make sure that the deviation of the averages from 1 really reflects the violation of isotropy, one can add small systematic anisotropy into the isotropic flow from the database [16] and watch what happens to the averages. For example, with this easy trick we 'model' an effect of a systematic shear by adding constant non-random addition  $\delta A_{12} = a$  (recall that  $A_{12} = u_x / y$ ). The result is presented in Fig. 3. One can see that the averages demonstrate qualitative behavior similar to that in Fig.2. Two of them increase, and two decrease; the average  $\langle s_1^{-2} s_2^{-2} s_3^2 \rangle$  and the two ' $y$ -axial' averages appear to be the least sensitive to the symmetry violation in both Figures. The similarity of the trends may indicate that near the wall, this 'shear' type of symmetry violation

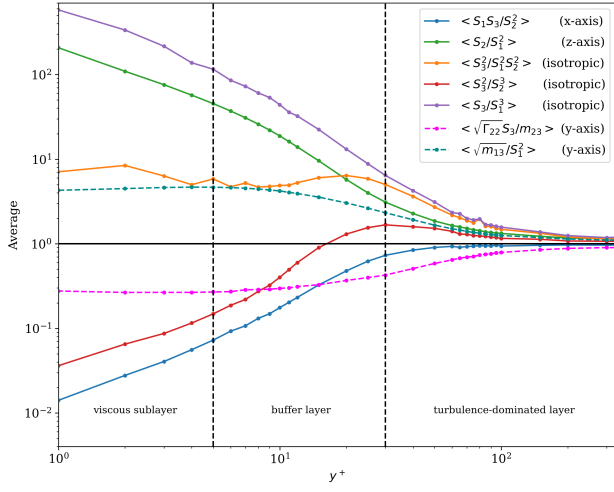


FIG. 2: The averages vs the wall-normal coordinate ( $y^+$ ). The three qualitatively different zones of a channel flow are shown by dashed lines.

plays an important role.

The sensitivity of the averages to the distortion of isotropy in Fig. 3 is notable: they deviate from the 'isotropic' value 1 by two times, while the rms value of  $A_{12}$  changes quite slightly. This demonstrates the good sensitivity of the averages to the violation of statistical isotropy.

One can find more graphs describing the dependence of the averages on different components of  $\mathbf{A}$  in Supplemental Material 2: every type of addition changes the curves crucially.

We note that, apart from stochastically isotropic tensors, the identities (8) are also fulfilled for tensors of the form  $\mathbf{B} = f(\mathbf{A})\mathbf{A}$  where  $\mathbf{A}$  is isotropic, and  $f(\mathbf{A})$  is a scalar anisotropic function of  $\mathbf{A}$  (e.g.,  $f(\mathbf{A})$  is some numerical function of components of  $\mathbf{A}$  in some chosen coordinate frame). [22] However, in real turbulence local anisotropy is due to a large-scale flow, and cannot take such form.

## CONCLUSION

The stochastic identities discussed in the paper are presented as the expectations of specific dimensionless combinations of random tensor components. If the tensor is stochastically isotropic, all the five expectations listed in Table 1 are equal to unity; moreover, every one of them generates a three-parametric family of identities. In presence of axial symmetry there are two one-parametric families.

The discovery of these identities was made possible by the works [12, 19]. While studying the evolution of coherent structures frozen into a random isotropic flow, we discovered a rather unexpected property of the evolution

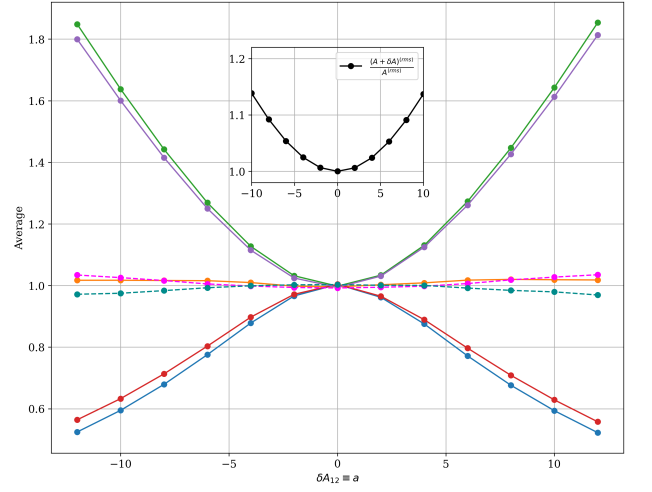


FIG. 3: 'Artificial shear-flow asymmetry': systematic non-random  $\delta A_{12} = a$  added to the isotropic dataset for velocity gradients. The inset shows  $a$  relation to the rms value of the velocity gradient.

matrix, and a series of new integrals of motion related to it. However, after further investigation it became clear that these properties are just as true for any stochastically isotropic tensor, not only for the evolution matrix. This paper states that the new non-trivial stochastic identities can be obtained for any second-rank tensor field associated with isotropic turbulent flow, and even for any stochastically isotropic second-rank tensor of any nature in a space of arbitrary dimension.

The application of the theory to the results of numerical simulations of incompressible turbulent flow, both isotropic and in the channel, demonstrates that the averages can be used as markers of isotropy. The analysis of the velocity gradient tensor shows that the cumulative averages converge well to definite values, isotropic turbulence and the center of the channel exhibiting averages close to unity, which confirms the theory. Near the wall, deviations from unity become much more pronounced, with axial symmetry holding further than other symmetries. The study also highlights the sensitivity of the averages to violation of isotropy; this is demonstrated by addition of small systematic anisotropy to the isotropic flow. Thus, the proposed method can be used in investigation of turbulent flows to estimate their deviation from idealized isotropic conditions, the violation of the identities being treated as the measure of this deviation.

We recall that the identities discovered in the paper are valid for any kind of tensors, for example, for magnetic induction gradients in MHD turbulence; and for different types of random fields, including non-stationary (in particular decaying) turbulence. This fact can also be validated by DNS or experiments.

Aside from being used as the markers of isotropy, these identities can also be helpful in considering the theoretic-

cal problems of the turbulence theory [3, 20, 21]. In this sense, we hope they can be as useful as, for instance, Ward identities have turned out to be in renormalized quantum electrodynamics. Furthermore, it may be possible to generalize the presented theory for other symmetry groups, in addition to  $O(d)$ . Studying the symplectic group from this angle, for example, may be useful in stochastic Hamiltonian mechanics and similar problems. However, all of these ideas, while promising, are just at the beginning of their development.

We thank both anonymous Referees for valuable remarks. The work of A.V.K. was supported by RSF grant No. 24-72-00068.

- 
- [1] A.N. Kolmogorov, The Local Structure of Turbulence in Incompressible Viscous Fluid for Very Large Reynolds Numbers, *Dokl. Akad. Nauk SSSR*, **30**, 299 (1941)
  - [2] U. Frisch, *Turbulence: the legacy of A.N. Kolmogorov.*, Cambridge Univ. Press, Cambridge (1995)
  - [3] A.S. Monin and A.M. Yaglom *Statistical Fluid Mechanics, Vol. 1.*, MIT Press, Cambridge (1975)
  - [4] S. Chowdhuri and T. Banerjee, Quantifying small-scale anisotropy in turbulent flows. *Phys. Rev. Fluids*, **9**(7), 074604 (2024)
  - [5] C. Meneveau, Lagrangian dynamics and models of the velocity gradient tensor in turbulent flows, *Annu. Rev. Fluid Mech.* **43**, 219 (2011)
  - [6] P.L. Johnson and M. Wilczek, Multiscale velocity gradients in turbulence, *Annu. Rev. Fluid Mech.* **56**, 463 (2024)
  - [7] A.A. Schekochihin, MHD turbulence: a biased review, *Jour. Plasma Phys.* **88**, 155880501 (2022)
  - [8] E.A. Kuznetsov and E.A. Mikhailov, Slipping flows and their breaking, *Ann. Phys.* **447**, 169088 (2022)
  - [9] G. Falkovich, K. Gawedzki and M. Vergassola, Particles and fields in fluid turbulence, *Rev. Mod. Phys.* **73**, 913 (2001)
  - [10] P.E. Dimotakis, Turbulent mixing, *Annu. Rev. Fluid Mech.* **37**, 329 (2005)
  - [11] F.G. Michalec, I. Fouxon, S. Souissi and M. Holzner, Zooplankton can actively adjust their motility to turbulent flow, *PNAS* **114**, E11199 (2017)
  - [12] V.A. Sirota, A.S. Il'yn, A.V. Kopyev and K.P. Zybin, Lagrangian stochastic integrals of motion in isotropic random flows, *Phys. Fluids* **36**, 021701 (2024)
  - [13] V.F. Kopyev and S.A. Chernyshev, Simulation of azimuthal characteristics of turbulent jet noise by correlation model of quadrupole noise sources, *Intern. Journ. Aeroacoustics*, **13**, 39 (2014)
  - [14] N. Nikitin, Turbulent secondary flows in channels with no-slip and shear-free boundaries, *Jour. Fluid Mech.* **917**, A24 (2021)
  - [15] V.S. Beskin, Magnetohydrodynamic models of astrophysical jets, *Physics-Uspekhi*. **53**(12), 1199 (2010)
  - [16] Y. Li et al, A public turbulence database cluster and applications to study Lagrangian evolution of velocity increments in turbulence, *Journ. Turbulence*, **9**, 31 (2008)
  - [17] J. Graham et al, A web services accessible database of turbulent channel flow and its use for testing a new integral wall model for LES, *Journ. Turbulence*, **17**(2), 181 (2016)
  - [18] E. Perlman, R. Burns, Y. Li and C. Meneveau, Data exploration of turbulence simulations using a database cluster, In *Proceedings of the 2007 ACM/IEEE Conference on Supercomputing*, pages 1-11 (2007)
  - [19] A.S. Il'yn, A.V. Kopyev, V.A. Sirota and K.P. Zybin, Material surfaces in stochastic flows: Integrals of motion and intermittency, *Phys. Rev. E* **107**, L023101 (2023)
  - [20] R.J. Hill, Equations relating structure functions of all orders, *J. Fluid Mech.* **434**, 379 (2001)
  - [21] V. Yakhot, Mean-field approximation and a small parameter in turbulence theory, *Phys. Rev. E* **63**, 026307 (2001)
  - [22] It was the Anonymous Referee who drew our attention to the fact.

## Supplemental Material

### Geometric interpretation of the stochastic identities

The identities derived in the paper can be described in geometric terms, in a way invariant with respect to the choice of coordinate frame. Every one of the five continuous families of identities then correspond to one and the same invariant geometric identity.

Consider random isotropic linear operator  $\mathcal{A}$  in Euclidean space  $\mathbb{R}^d$  and an arbitrary ordered set of orthonormal vectors  $\{\mathbf{e}_1, \mathbf{e}_2, \dots, \mathbf{e}_d\}$ .

The sequence of sets of vectors

$$\mathbf{e}_1, \quad \{\mathbf{e}_1, \mathbf{e}_2\}, \quad \dots \quad \{\mathbf{e}_1, \mathbf{e}_2, \dots, \mathbf{e}_d\}$$

is called a flag. It corresponds to a set of parallelepipeds of different dimensions, each one embedded in the next one.

The action of  $\mathcal{A}$  transforms the initial flag into random flag:

$$\mathcal{A}\mathbf{e}_1, \quad \{\mathcal{A}\mathbf{e}_1, \mathcal{A}\mathbf{e}_2\}, \quad \dots \quad \{\mathcal{A}\mathbf{e}_1, \mathcal{A}\mathbf{e}_2, \dots, \mathcal{A}\mathbf{e}_d\}$$

We are interested in the length of the first vector  $L = \|\mathcal{A}\mathbf{e}_1\|$ , the square of the parallelogram  $S = \|\mathcal{A}\mathbf{e}_1 \wedge \mathcal{A}\mathbf{e}_2\|$  and the rest of the hypervolumes of the flag elements. Since  $\mathcal{A}$  is a random operator, these hypervolumes are also random; however, because of isotropy of  $\mathcal{A}$ , the probability density of  $L$  does not depend on the direction of  $\mathbf{e}_1$ . Likewise, the joint probability density  $\rho(L, S, \dots)$  of  $L$ ,  $S$  and other hypervolumes does not depend on the choice of the vectors  $\{\mathbf{e}_1, \mathbf{e}_2, \dots, \mathbf{e}_d\}$ . Nor do different moments of these values depend on the initial orthonormal flag.

If the set of vectors that generate the initial flag  $\{\mathbf{e}_1, \mathbf{e}_2, \dots, \mathbf{e}_d\}$  coincides with the standard basis, we find out that the hypervolumes of the resulting flag are related to the minors of the matrix representation of  $\mathbf{\Gamma} = \mathcal{A}^T \mathcal{A}$  in the standard basis :

$$L = s_1, \quad S = s_2, \quad \dots$$

Thus, the five identities listed in Table 1 of the paper can be interpreted as five nontrivial stochastic properties of the flag's hypervolumes.

If the set of the flag-generating vectors does not coincide with the standard basis, the same geometric properties of the flag are still valid and bring new algebraic identities for any choice of the initial flag. Thus, rotating the initial flag (i.e., the set  $\{\mathbf{e}_i\}$ ) one gets a three-parametric family of algebraic identities for each of the original five (or  $d! - 1$  identities each of them being  $d(d-1)/2$ -parametric in general case).

### Distortion of isotropy

To illustrate the sensitivity of the averages to different types of isotropy distortion, a series of graphs is presented in Figure 4. The graphs in the first and the second row represent fixed shears over isotropic turbulence gradients, i.e. sequentially introduce addition of various off-diagonal components to the velocity gradients tensor. The graphs in the third row represent stretched incompressible cylinder over isotropic turbulent flow, i.e. introduce diagonal components while maintaining the incompressibility condition. Note that for distortions that preserve the axial symmetry with respect to  $x$ -axis or to  $z$ -axis, the corresponding averages remain unity.

---

[1] Y. Li et al, Journ. Turbulence, **9**, 31 (2008)

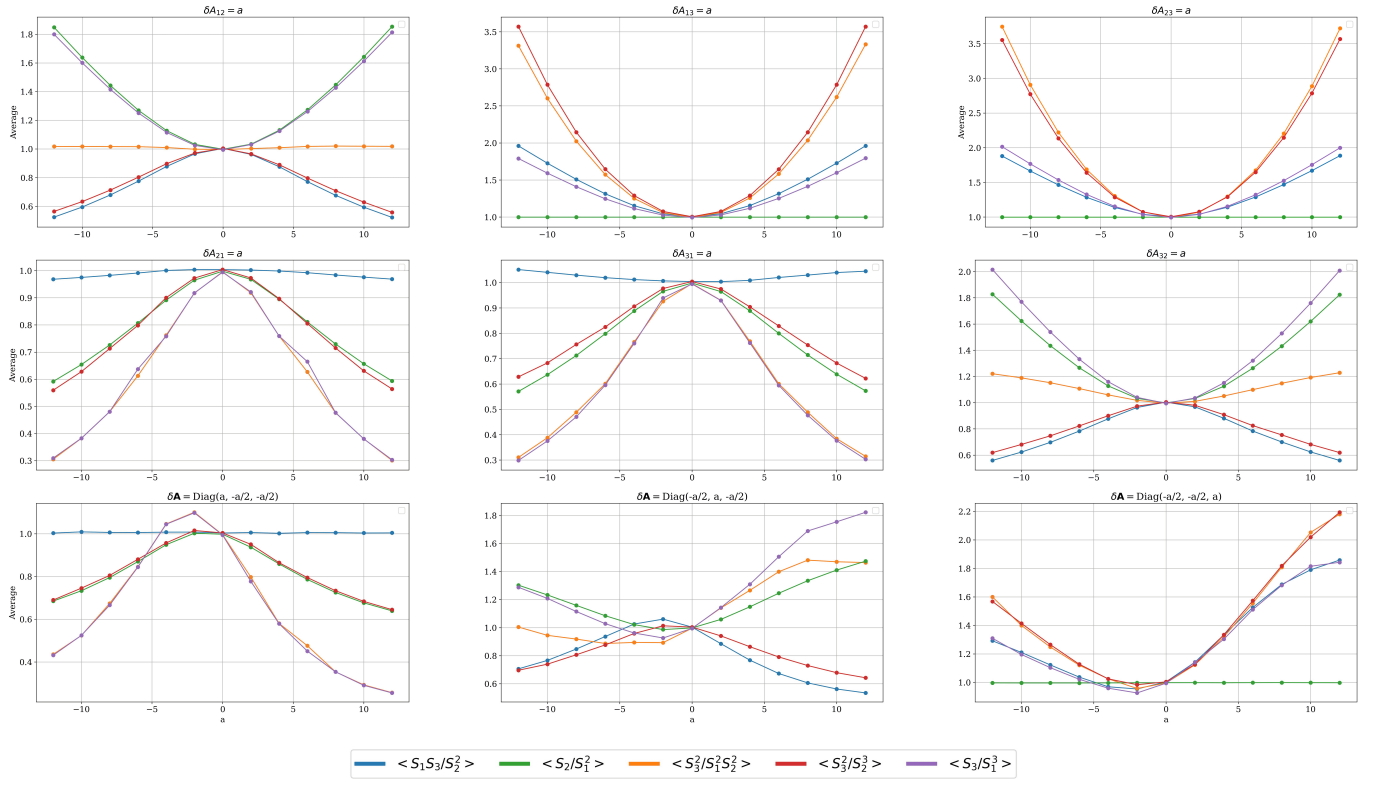


FIG. 4: 'Artificial shear-flow asymmetry': dependence of the averages on systematic non-random velocity gradients that distort the isotropic dataset [1]. The type of distortion is written in the title of every graph. The legend for the averages is placed below the graphs.